



OPEN Cold environment regulates ischemic stroke through modulation of gut microbiota

Xiao Zhou^{1,4}, Chanjuan Wei^{1,4}, Jiaming Liu^{1,4}, Xiaoshuang Xia¹, Lin Wang² & Xin Li^{1,3}✉

Many diseases are influenced by environmental temperature, and recent studies have confirmed that cold exposure increases the risk of conditions such as ischemic stroke (IS). However, direct evidence supporting this hypothesis is lacking, and the molecular mechanisms through which cold exposure affects IS remain unclear. In this study, we found that chronic cold exposure increased platelet aggregation and the levels of certain inflammatory factors in high-risk stroke patients (HR), thereby increasing the risk of IS. Furthermore, before and after a cold wave, we observed gut microbiota dysbiosis in the HR group, including reduced relative abundance differences in *Lachnospiraceae* and *Ruminococcaceae*. The relative abundances of the *Prevotella_9* and *Catenibacterium* genera increased, whereas that of *Anaerostipes* decreased. Notably, the results of fecal microbiota transplantation (FMT) indicated that cold-adapted microbiota transplantation partially replicated the microbiota characteristics of each donor subject and replicated the effects of cold exposure in C57BL/6J mice. Cold exposure impaired intestinal barrier function and interfered with microbial functions, such as increased lipid metabolism and LPS production, particularly by increasing the levels of TMAO derived from the gut microbiota. Our findings identify the significant role of abnormal gut microbiota-derived metabolites in cold exposure-related IS and highlight the potential opportunity to prevent or treat cold-related IS through the modulation of the gut microbiota.

Keywords Cold temperature, Ischemic stroke, Microbiota, TMAO

The environmental temperature has a significant effect on the physiology and pathology of mammals. Physiologically, when mammals are exposed to cold or hot environments, temperature receptors detect external stimuli and transmit information to the hypothalamus, triggering responses such as skin vasodilation and shivering to generate heat, thereby helping to regulate core body temperature^{1,2}. In addition to heat-producing responses, environmental temperature influences other physiological and morphological characteristics in mammals, such as myocardial cell damage, disruption of ion channel functions in myocardial cell membranes, and hormonal imbalances³. Furthermore, exposure to extreme temperatures can affect the onset and progression of various diseases, including obesity, hypertension, heart failure, preeclampsia, and cancer, and may even lead to death^{4–7}.

Stroke is a leading cause of death and disability in China, ranking second globally⁸. With global warming and the increasing frequency of extreme weather events such as cold waves and heatwaves, exposure to nonoptimal environmental temperatures is becoming an increasingly serious threat to the cardiovascular system^{9,10}. In recent decades, accumulating epidemiological evidence has shown that environmental temperature is closely related to the increased incidence and mortality of cerebrovascular diseases¹¹. In many countries and regions, exposure to both low and high temperatures can lead to an excess of stroke events¹². The Global Burden of Diseases, Injuries, and Risk Factors Study (GBD) indicated that in 2019, the number of stroke disability-adjusted life years (DALYs) related to low environmental temperatures reached 8.36 (6.19–10.80) million, whereas the number of stroke DALYs related to high environmental temperatures was 1.09 (0.11–2.38) million¹². In most regions of the world, cold effects dominate, but in areas with relatively high prevailing temperatures, heat effects may far exceed cold effects. The results of these retrospective and prospective epidemiological studies provide evidence for the association between cold exposure and IS. Although many studies have explored the relationship between cold exposure and IS, the molecular mechanisms underlying the harmful effects of cold exposure on IS remain unclear.

¹Department of Neurology, The Second Hospital of Tianjin Medical University, No. 23, Pingjiang Road, Tianjin 300211, China. ²Department of Geriatrics, The Second Hospital of Tianjin Medical University, Tianjin, China. ³Tianjin Center for Health and Meteorology Multidisciplinary Innovation, Tianjin, China. ⁴Xiao Zhou, Chanjuan Wei and Jiaming Liu equally contributed to this work. ✉email: lixinshi@126.com

Over the past decade, it has become clear that the residents of our gut, the gut microbiota, play crucial roles in human metabolism, immune function, and the body's response to diseases, including IS¹³. The gut microbiota can regulate risk factors for vascular diseases such as hypertension, diabetes, obesity, and hyperlipidemia and can promote atherosclerosis by increasing the levels of trimethylamine N-oxide (TMAO)¹⁴. Additionally, changes in the gut microbiota significantly impact the immune response related to IS, the severity of the condition, and the prognosis. This microbial imbalance may result from gut ischemia-reperfusion events triggered by IS, including an abnormal increase in Enterobacteriaceae within the gut¹⁵. This increase can further stimulate systemic inflammatory responses, thereby exacerbating stroke damage. Furthermore, cold stress affects the gut microbiota. Studies have shown that mice exposed to cold environments exhibit reduced gut microbial diversity, a decreased Firmicutes/Bacteroidetes (F/B) ratio, and a reduced relative abundance of Verrucomicrobia¹⁶. A recent study successfully established a cold-induced hypertension (CIH) model and revealed that cold exposure reduced the diversity of the gut microbiota; increased the abundance of pathogenic bacteria (such as *Quinella*, *Rothia*, and *Senegalimassilia*); and decreased the abundance of beneficial bacteria (such as *Lactobacillus*) and bacteria producing short-chain fatty acids (such as *Lachnospiraceae* UCG-008 and *Ruminococcaceae* UCG-013)¹⁷. Therefore, we hypothesize that there is a complex and close relationship between cold exposure, the gut microbiota, and IS.

The identification of microbial-derived metabolites can provide insights into how the gut microbiota regulates the development of host diseases and assist in the screening of potential therapeutic molecules¹⁸. In this study, we explored the impact of cold exposure on stroke-prone populations. To better characterize the stroke risk associated with cold exposure, we assessed a panel of circulating biological indicators that may reflect inflammatory status, platelet reactivity, and endothelial function. These included intercellular adhesion molecule-3 (ICAM-3), lipoprotein-associated phospholipase A2 (Lp-PLA2), tumor necrosis factor receptor 2 (TNFR2), vascular endothelial growth factor (VEGF), systemic immune-inflammation index (SII), and ADP-induced platelet aggregation receptors (PARs). These biomarkers have been implicated in stroke pathophysiology and may serve as early indicators of vascular dysfunction^{19–22}. Through gut microbiota analysis, antibiotic treatment, and fecal microbiota transplantation (FMT) experiments, we confirmed that cold exposure may exacerbate IS risk in high-risk mice by altering the composition of the gut microbiota. Furthermore, analysis via metagenomic approaches revealed that cold exposure led to lipid metabolism disruption and increased levels of LPS. Our findings provide new experimental evidence supporting the view that cold exposure exacerbates ischemic stroke and suggest that modulating the gut microbiota may hold potential for preventing and treating stroke in populations exposed to cold environments.

Methods

Clinical data

Study area and time series

This study was conducted in Tianjin, China, which is located in the northern part of the country (latitude 38°34'–40°15' N, longitude 116°43'–118°4' E). Tianjin experiences a warm temperate semihumid monsoon climate characterized by distinct seasons. The Tianjin Meteorological Bureau provided daily meteorological data for Tianjin from September 2022 to January 2023, including daily maximum temperature (Tmax) and minimum temperature (Tmin). The study period was divided into 24 solar terms of the Chinese lunar calendar. The results were compared by grouping them according to these solar terms^{23,24}.

Study design and proportions

The study participants were recruited from the Neurology and Geriatrics Department of the Second Hospital of Tianjin Medical University in September 2022. Fecal and blood samples were collected from the participants at three time points: September 2022, November 2022, and January 2023. All participants signed informed consent forms. This study adhered to the principles outlined in the Declaration of Helsinki, and received approval from the Ethics Committee of the Second Hospital of Tianjin Medical University (Approval No. KS20220901). All methods in our study performed in accordance with the relevant guidelines and regulations, and the study is reported in accordance with ARRIVE guidelines. Written informed consent was obtained from all participants' parents/guardians prior to their participation in the study.

The Essen stroke risk score (ESRS) ranges from 0 to 9 points, with higher scores indicating a greater risk of ischemic stroke²⁵. The participants were divided into two groups: those with an ESRS score of 3 or higher were classified into the high-risk group (HR), and those with a score lower than 3 were classified into the low-risk group (LR). All participants were screened by three senior neurologists. The inclusion criteria for the HR and LR groups are shown in the Supplementary material (1).

Stroke risk measures

The primary objective of this study was to evaluate changes in stroke risk among participants. In previous studies, the following indicators were assessed: ICAM-3, Lp-PLA2, TNFR2, and VEGF in the blood. Additionally, we analyzed changes in the SII and ADP-induced PARs. There is a significant association between the SII and the incidence of ischemic stroke^{26,27}.

Animal experiments

Male C57BL/6J mice (20–22 g) were purchased from Charles River Laboratories. Previous studies have shown that cold exposure does not significantly affect the platelet function of female C57BL/6J mice. To reduce confounding factors, male C57BL/6J mice were selected as the primary subjects for this study²⁸.

Fecal bacteria transplantation (FMT)

In this part of the study, we selected fecal samples from HR group participants who met the following criteria to minimize potential confounding factors: (1) aged over 75 years, (2) had a history of both hypertension and diabetes, and (3) did not have a history of heart disease. The detailed method of FMT is provided in the supplementary materials 3 and sfig3²⁹. The mice were divided into two specific groups: the CEHR group, in which the mice were transplanted with fecal samples from HR group participants after a cold wave (January 2023), and the NTHR group, in which the mice were transplanted with fecal samples from HR group participants during the baseline period (September 2022).

Platelet function

Blood was collected from the abdominal aorta of the mice under anesthesia (0.2 mL/10 g avertin) via a 1 mL syringe prefilled with 3.8% sodium citrate as an anticoagulant (whole blood:anticoagulant ratio = 9:1). The blood was centrifuged at 300 × g for 2 min at room temperature to separate the platelet-rich plasma (PRP). The PRP was further centrifuged at 700 × g for 2 min to pellet the platelets, which were then resuspended in Tyrode's buffer and adjusted to a concentration of 3×10^8 /mL. Platelet aggregation assays were conducted via a lumiaggregometer (Model 700; Chrono-Log, USA) and AggRAM™ (Helena, USA). Aggregation was initiated with different agonists (ADP, collagen, and thrombin) under stirring conditions (900 rpm), and the results were recorded. For the clot retraction assays, 300 µL of washed platelets from the four groups were aliquoted into cuvettes and mixed with 10 µL of human platelet-poor plasma (PPP). Clot retraction was initiated by adding 0.1 U/mL thrombin. The size of the clots at each time point was quantified via ImageJ software.

Immunohistochemistry

Sections of colon tissue embedded in paraffin were deparaffinized with xylene, followed by dehydration with alcohol. Antigen retrieval was performed in citrate buffer (pH 6.0). The sections were treated with 0.3% hydrogen peroxide to block endogenous peroxidase activity and blocked with 5% normal goat serum for 1 h. The sections were incubated overnight with primary antibodies against ZO-1 (1:300, Proteintech, Wuhan, China) and Occludin (1:300, Proteintech, Wuhan, China). The sections were washed in PBS. After the excess liquid was shaken, enhancer solution was applied within the ring to cover the tissue for 20 min. The sections were washed twice with PBST and once with PBS. After the excess liquid was shaken, the enhanced enzyme-linked polymer was applied within the ring to cover the tissue for 20 min. DAB was used for color development, and hematoxylin was used as a counterstain. The sections were dehydrated, and the slides were mounted. The tissue samples were imaged via an Olympus BX46 microscope (Olympus, Japan). The staining intensity was quantified via Image-Pro Plus software.

Microbiota analysis

16S rRNA sequencing

According to the manufacturer's instructions, genomic DNA from the stool samples was extracted via the PF Mag-Bind Stool DNA Kit (Omega Biotek, Norcross, GA, USA). The final DNA concentration and purity were assessed via a NanoDrop 2000 UV-Vis spectrophotometer (Nanodrop Technologies, Wilmington, DE, USA). 16S rRNA gene sequencing was conducted by Majorbio Bio-Pharm Technology Co., Ltd. in Shanghai, China. The primers 515F and 806R were used to target the hypervariable V3 and V4 regions of the 16S rRNA gene for amplification. Following the protocol provided by Promega (Madison, WI, USA), the purity and concentration of the amplified products were measured via QuantiFluor™-ST. These amplicons were then pooled in equimolar amounts and sequenced on an Illumina MiSeq platform for a 300 bp paired-end read, following the standard procedures of Majorbio.

Metagenomic sequencing

Following the manufacturer's recommendations, total DNA from mouse stool was extracted via the MolPure® Stool DNA Kit (Yeasen, Shanghai, China). After DNA extraction, the concentration and purity were measured, and DNA integrity was assessed via 1% agarose gel electrophoresis. The DNA was then fragmented via a Covaris M220 (Covaris Inc., Woburn, Massachusetts, USA), and fragments of approximately 350 bp were selected for paired-end (PE) library construction. The library was prepared via the NEXTFLEX Rapid DNA-Seq Kit (Bioo Scientific, USA). Sequencing was performed on the Illumina NovaSeq™ X Plus platform (Illumina, USA) for metagenomic analysis.

Statistics

This study used SPSS version 26.0 (SPSS Inc., Chicago, Illinois, USA) and GraphPad Prism version 10.0 (GraphPad Software, San Diego, California, USA) for data analysis. The normality of numerical variables was assessed using the Shapiro–Wilk test. Data with a normal distribution were presented as mean ± standard deviation (SD), and within-group differences were evaluated using one-way analysis of variance (ANOVA), followed by Tukey's test for post-hoc pairwise comparisons. Data that did not meet the normality assumption were presented as median (P25, P75), and within-group differences were analyzed using the non-parametric Kruskal–Wallis test, followed by Dunn's test for post-hoc pairwise comparisons. All images related to gut microbiome analysis were created via the R software package and GraphPad Prism 10 (GraphPad Software, San Diego, California, USA), with data organization completed via the tidyverse collection of packages in R.

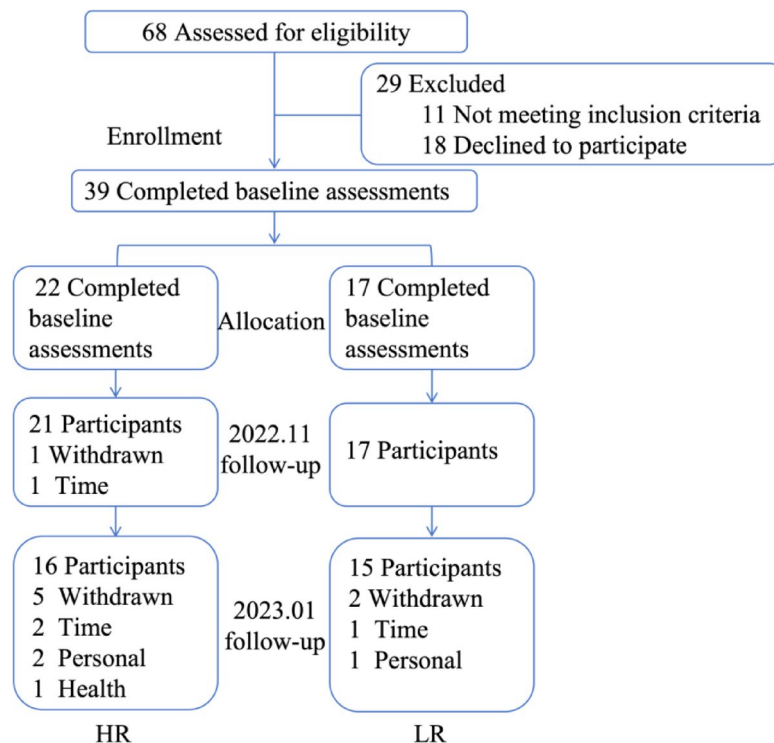


Fig. 1. The flowchart for the study.

Variables	HR group (n = 22)	LR group (n = 17)
Age [years]	71.09 ± 8.09	66.71 ± 4.99
Female	7 (31.8%)	6 (35.3%)
Current smoking (%)	15 (68.2%)	4 (23.5%)
Alcohol (%)	8 (36.3%)	2 (11.8%)
Hypertension (%)	20 (91.1%)	8 (47.1%)
t2DM (%)	10 (45.6%)	3 (17.6%)
Previous stroke	9 (40.9%)	0 (0%)
Other cardiovascular diseases	8 (36.4%)	2 (11.8%)
Peripheral arterial disease	4 (18.2%)	1 (5.9%)
Hyperlipidemia	10 (45.6%)	6 (35.3%)
SII	1334.21 (743.66, 1477.82)	903.5 ± 377.04

Table 1. Baseline characteristics of the two groups. At baseline, the means and standard deviations of the scores represented normally distributed data, and the data that were not normally distributed were described as medians and interquartile ranges (IQRs).

Results

Clinical data

Basic information of the participants and meteorological data

The recruitment period for participants was from September 2022 to January 2023. The process flow for participants in the study is illustrated in Fig. 1. A total of 68 participants were enrolled and underwent baseline assessment. A total of 31 participants (16 in the HR group and 15 in the LR group) completed the 5-month follow-up. Baseline characteristics are shown in Table 1. The temperature changes are shown in Fig. 2.

Changes in plasma markers after the cold wave

To assess the impact of chronic cold waves on the risk of IS, we analyzed changes in several biomarkers (sTable1). Before and after exposure to cold waves, the HR group presented a significant increase in IS risk, with ADP-induced platelet aggregation rates (PARs) and ICAM-3 and VEGF levels markedly elevated (Fig. 3A–C). In contrast, while biomarkers in the LR group tended to increase, the changes did not reach statistical significance (Fig. 3). In the analysis of the SII, although both groups showed an increasing trend in the SII from pre- to

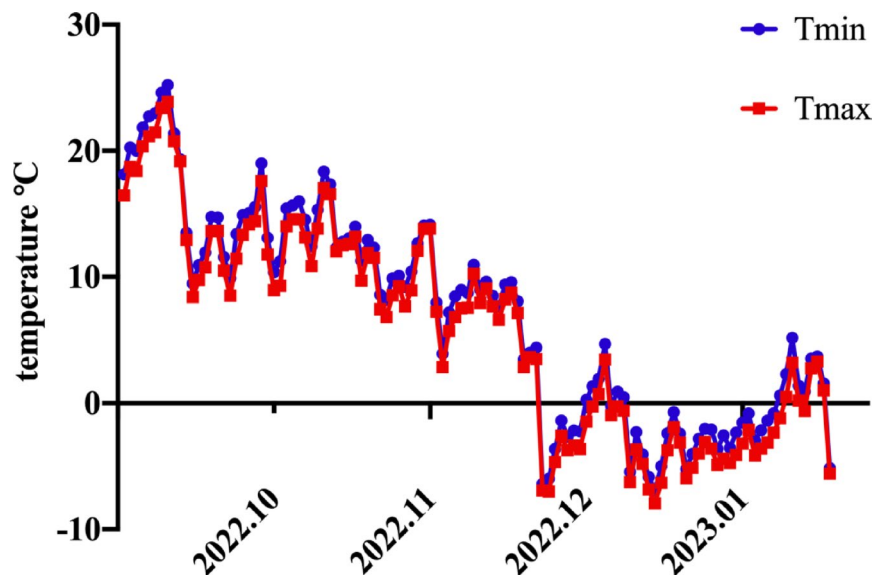


Fig. 2. Temperature changes during the study period.

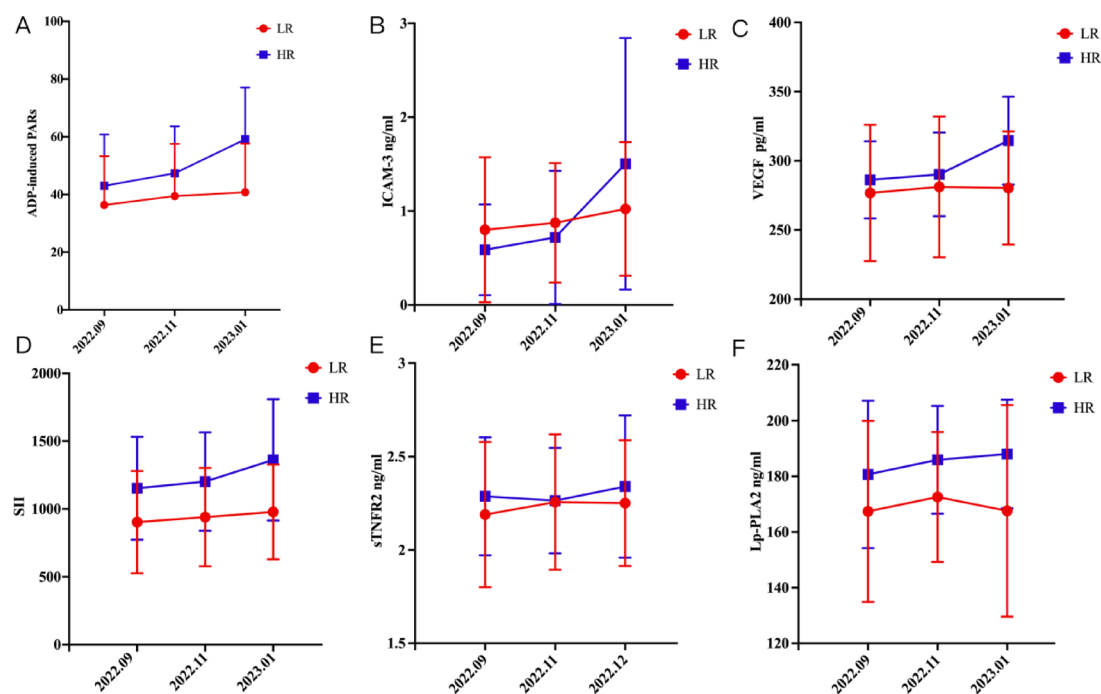


Fig. 3. Changes in primary outcomes after experiencing a cold wave. (A) Effects of cold waves on ADP-induced PARs. (B) Effects of cold waves on ICAM-3. (C) Effect of cold waves on VEGF. (D) Effect of cold waves on SII. (E) Effect of cold waves on sTNFR2. (F) Effects of cold waves on the Lp-PLA2S.

postfollow-up, no significant changes were observed (Fig. 3D). However, there were no significant changes in sTNFR2 and Lp-PLA2 levels in both groups (Fig. 3E,F).

Changes in the composition of the gut microbiota after the cold wave

Recent evidence suggests that gut dysbiosis is associated with the occurrence of stroke³⁰. To investigate whether cold waves alter the gut microbiota composition in the HR and LR groups, we performed 16S ribosomal DNA analysis on the microbiota from participants' fecal samples. After the cold wave, the α diversity of the gut microbiota in the HR group tended to decrease, with a significant decrease in the ACE index (Fig. 4A) but no significant differences in the Shannon or Chao diversity (Fig. S1A and B). No significant differences were detected in the LR group (Fig. 4B). We then performed principal coordinate analysis (PCoA) to examine the impact of cold

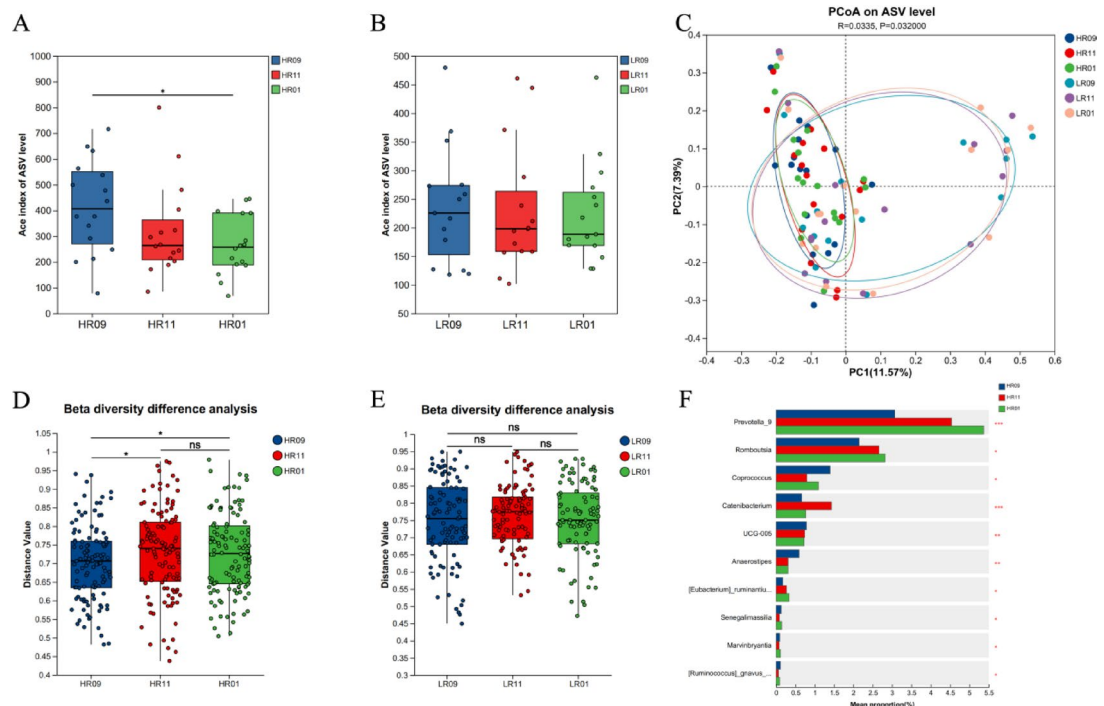


Fig. 4. (A, B) Alpha diversity of the HR and LR group. (C) Principal coordinate analysis (PCoA) plot based on the Bray–Curtis distance matrix depicting patterns of beta diversity from the gut microbial communities at the ASV level. (D, E), Based on the beta diversity distance among samples within each group, we analyzed the differences in sample distances at different times within the HR and LR groups to compare differences in community structure between groups. (F) Figure showing the 10 differential genera among HR group (Kruskal–Wallis test with Dunn’s post-hoc test, and FDR correction for multiple comparisons was applied, with a significance threshold of 0.05).

exposure on the overall microbiota composition. No significant changes in β diversity were observed in either the HR or LR groups after the cold wave (Fig. 4C). However, the results of the β diversity differential analysis revealed that the degree of dispersion and heterogeneity within the HR group was significantly greater than that within the LR group (Fig. 4D,E), indicating that cold exposure has a significant effect on the composition of the gut microbiota. At the genus level, the relative abundance of microorganisms further supported the changes in the gut microbiota composition. The relative abundances of the *Prevotella_9*, *Romboutsia*, and *Catenibacterium* genera significantly increased in the HR group after the cold wave, whereas those of the *Coproccoccus*, *UCG-005*, and *Anaerostipes* genera significantly decreased in the HR group following the cold wave (Fig. 4F).

Animal experiments

Platelet function after fecal bacterial transplantation

Light transmission aggregometry is the gold standard for evaluating platelet function and has been widely used. Therefore, we explored the effects of cold exposure on mouse platelets via light transmission aggregometry. Compared with those in the NTHR group, the rates of platelet aggregation induced by ADP (5 μ M), thrombin (0.02 U/mL), and collagen (1 μ g/mL) were significantly greater in the CEHR group (Fig. 5A). Clot retraction is one of the indicators reflecting the state of platelet activation (Fig. 5B). Our study revealed that, compared with those in the NTHR group, the clot retraction ability of the mice in the CEHR group was greater.

Colonic injury

To evaluate changes in intestinal homeostasis, considering that tight junctions are crucial for epithelial barrier function, we assessed the differential expression of the tight junction proteins Occludin and ZO-1. Positive staining for Occludin and ZO-1 was mainly observed between epithelial cells on the surface of the colon and those lining the crypts, with brownish staining indicating positive expression of Occludin and ZO-1. The staining intensity score (none=0, weak=1, moderate=2, strong=3) multiplied by the positive percentage score (no staining=0, staining less than 25%=1, 25%–50% staining=2, 50%–75% stained cells=3, staining over 75%=4) constituted the final IHC score for the samples. The results revealed that the positive expression of tight junction proteins (Occludin and ZO-1) was significantly lower in the CEHR group than in the NTHR group (Fig. 6).

Gut microbial composition and function of the CEHR and NTHR groups

We compared the gut microbiomes of the CEHR and NTHR groups. The PCoA plot based on the genus-level relative abundance distribution revealed that axis 1 (PCoA1) explained 32.5% of the variability, and axis 2

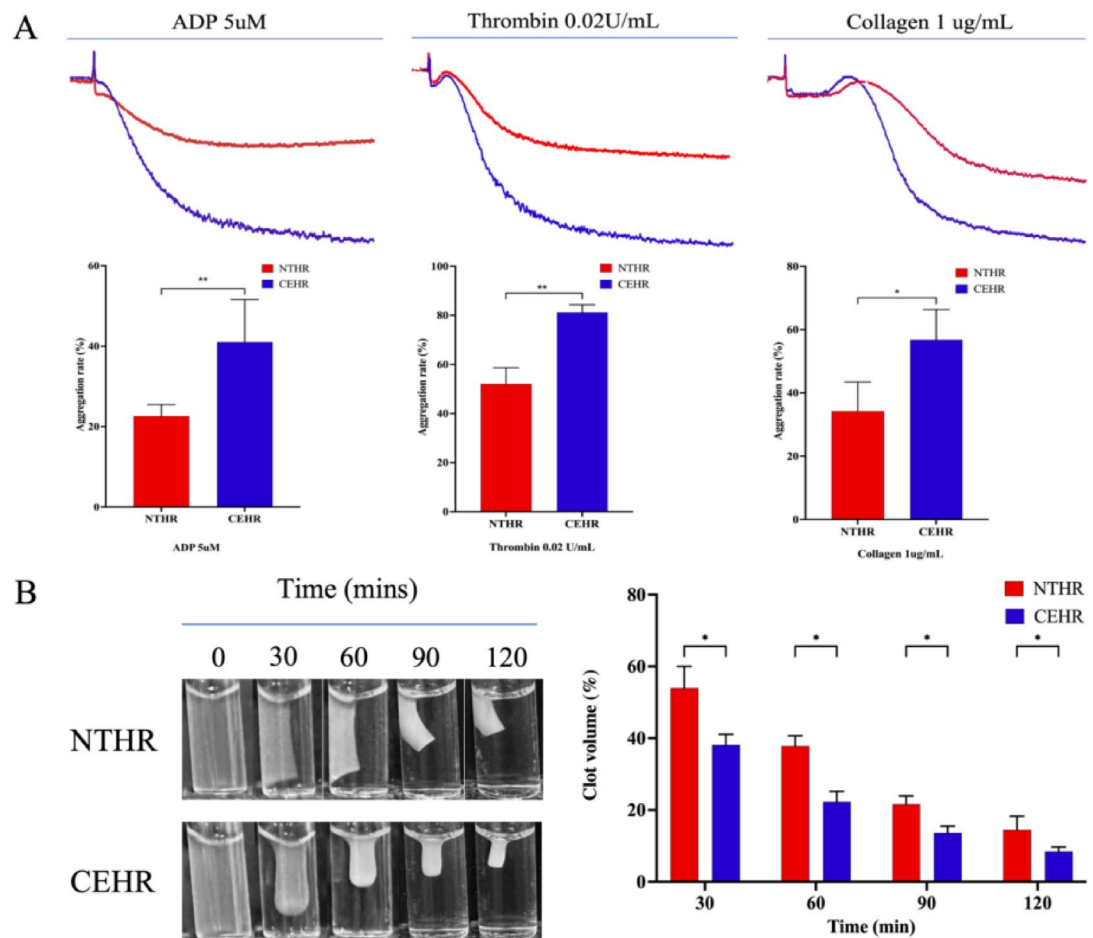


Fig. 5. Cold exposure promotes platelet activation. **(A)** Cold exposure promotes platelet aggregation induced by different agonists. At 37 °C, different concentrations of ADP (5 μ M, $n=6$), thrombin (0.02 U/mL, $n=5$), and collagen (1 μ g/mL, $n=5$) were used to stimulate washed platelets in mice. A Chrono-log lumi-aggregometer and AggRAM™ are used to record platelet aggregation continuously for 180 s. **(B)** Cold exposure promotes the clot retraction ability of platelets. Clot retraction of washed platelets from the NT and CE groups triggered by 0.1 U/mL thrombin ($n=6$). Photographs were taken at the indicated times. The sizes of the clots were quantified via ImageJ software.

(PCoA2) explained 27.2% of the variability. The PCoA plot indicated that the samples from the CEHR and NTHR groups were almost completely separated (Fig. 7A). The results revealed that there were 6 dominant phyla with relative abundances exceeding 1% in at least one sample: *p__Actinomycetota* (0.8–30.0%), *p__Bacillota* (0.7–28.9%), *p__Bacillota_A* (3.6–15.1%), *p__Bacteroidota* (2.9–16.6%), *p__Pseudomonadota* (0.81–23.4%), and *p__Verrucomicrobiota* (0.01–32.6%) (Fig. 7B). The gut microbiome of the NTHR group was dominated by *Ligilactobacillus* (35.04%), *Muribaculum* (11.89%), *Duncaniella* (9.75%), *Dubosiella* (9.04%), *Akkermansia* (9.80%), *Bacteroides* (7.05%), and *Bifidobacterium* (5.18%). In contrast, the gut microbiome of the CEHR group was enriched with *Muribaculum* (33.17%), *Akkermansia* (23.24%), *Lepagella* (9.7%), and *Bacteroides* (7.96%) (Fig. 7C). We used LEfSe to compare the relative abundances of gut bacteria at the genus level between the two groups. Only five genera were significantly more abundant in the CEHR group. In contrast, more genera, such as *g__Mucispirillum*, *g__Acetatifactor*, and *g__Intestinimonas*, were enriched in the NTHR group ($p < 0.05$, LDA > 2) (Fig. 7D). At the species level, there were also significant differences in microbial species between the two groups (Fig. 7E).

The abundances of microbial gene families and metabolic pathways were quantified via HUMAnN3 to compare the functional differences in the gut microbiome. A PCoA plot based on gene family abundance revealed that the samples from the NTHR and CRHR were almost completely spatially separated (Fig. 8A). Notably, the metabolic pathways of the CEHR gut microbiome were enriched in LPS biosynthesis. The metabolic pathways of the NTHR gut microbiome were enriched in the production of SCFAs (Fig. 8B).

To further characterize the overall functions of the gut microbiome, we predicted the gene functions of the gut microbiome on the basis of the KEGG database^{31–33}. The most abundant genes in both groups were related to metabolism, particularly lipid metabolism, amino acid metabolism, cofactor and vitamin metabolism, and energy metabolism. At level 3, inflammation-related pathways, such as lipopolysaccharide biosynthesis, and lipid metabolism-related pathways, such as arachidonic acid metabolism and linoleic acid metabolism,

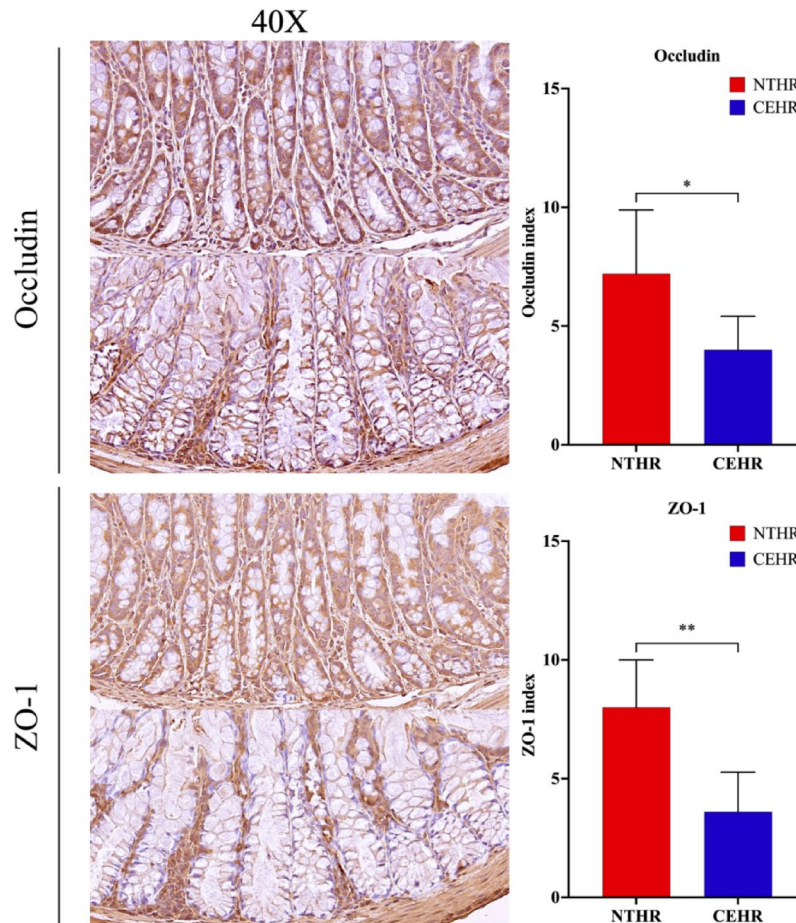


Fig. 6. Immunohistochemical staining and quantification of Occludin and ZO-1 in colon tissue samples from the NTHR (n=5) and CEHR (n=5) groups.

were significantly enriched in the CEHR group. Moreover, propanoate metabolism and ascorbate and aldarate metabolism were more enriched in the NTHR group (Fig. 8C,D).

Effects of LPS incubation on platelet function in vitro

On the basis of the gut microbiota metagenomic results, we further conducted in vitro experiments to investigate the impact of LPS on platelet function.

Fecal LPS levels after fecal microbiota transplantation Lipopolysaccharide (LPS), a major pathogen-associated molecular pattern (PAMP) secreted by pathogenic bacteria, is released under various stress conditions, such as temperature changes (e.g., cold exposure) and tissue injury. Extracellular LPS can bind to receptors such as TLR4 and MD2, triggering inflammatory responses. We measured the fecal LPS levels in the CEHR and NTHR mice after FMT and found that the LPS level was significantly elevated posttransplantation (Fig. 9A).

LPS enhances platelet function in vitro The results demonstrated that, compared with the control group (sterile PBS), in vitro incubation with 1 µg/mL LPS significantly enhanced platelet aggregation induced by ADP (5 µM), thrombin (0.02 U/mL), and collagen (1 µg/mL) compared with that in the control group (Fig. 9B). Additionally, LPS (1 µg/mL) accelerated clot retraction in platelets (Fig. 9C).

Discussion

Hippocles (approximately 400 BCE) reported that many illnesses were linked to weather conditions. The impact of climate change on public health occurs in part through extreme weather events such as cold waves, heatwaves, and floods, which directly affect human health. Among the meteorological factors, temperature is one of the most significant influences on health. When the temperature fluctuates abnormally, the body's ability to regulate itself and maintain thermal balance is disrupted, leading to discomfort and potentially causing illnesses³⁴. In our study on temperature and humidity control, cold exposure was found to increase the risk of IS onset^{35,36}. However, the role of cold exposure in the pathogenesis of IS remains controversial. Our experimental research provides strong evidence that strongly supports the long-standing view that cold weather has a detrimental effect on IS, and we recommend that individuals at high risk for IS avoid exposure to cold environments.

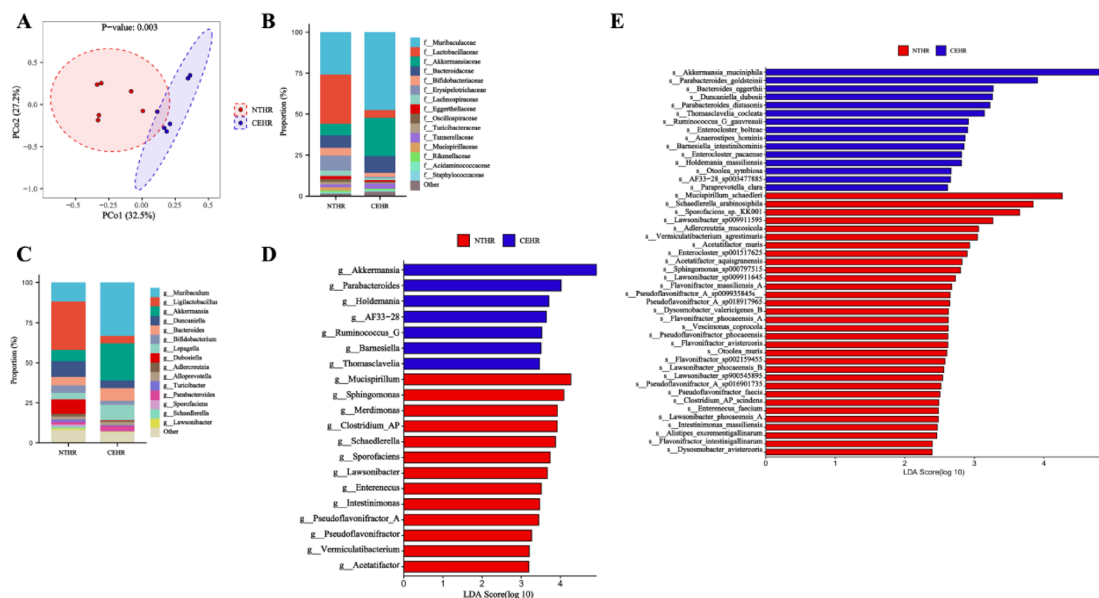


Fig. 7. The gut microbiome composition of the NTHR and CEHR groups. (A) PCoA plot based on the Bray-Curtis distance of the genus-level relative abundance profile ($p = 0.003$). (B) Bar chart showing the phylum-level composition of the gut microbiome. (C) Bar chart showing the genus-level composition of the gut microbiome (D). The difference in genus-level relative abundance according to LEfSe ($p < 0.05$ and $LDA > 2$). E. Differences in species-level relative abundance according to LEfSe ($p < 0.05$ and $LDA > 2$).

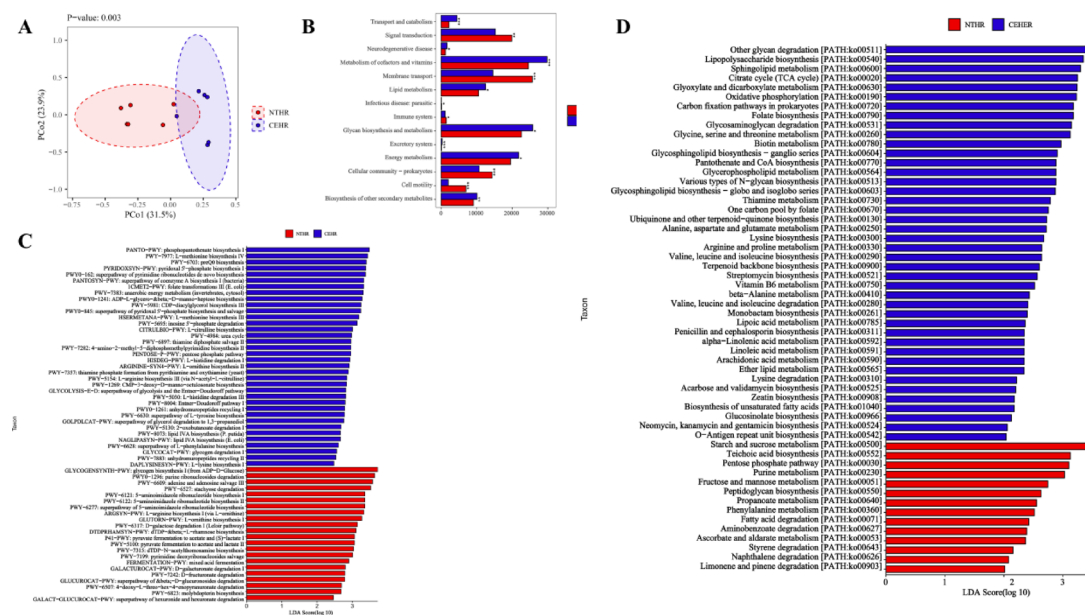


Fig. 8. (A) PCoA plot based on the Bray-Curtis distance of gene-family abundance ($p = 0.003$). (B) Differences in metabolic pathway abundance according to LEfSe ($p < 0.05$ and $LDA > 2$). (C, D) Comparison of the main KEGG functions (LEfSe, $p < 0.05$ and $LDA > 2$).

In the clinical study, the results revealed that after the cold wave, the change in stroke incidence risk was more significant in the high-risk (HR) group, with significant increases in ADP-induced PARs, ICAM-3, and VEGF levels. Although the low-risk (LR) group did not show significant changes, a similar upward trend was observed. Previous studies on the impact of short-term cold exposure on cardiovascular disease risk factors also indicated that, compared with the normal temperature group, the release of thromboxane B2 (TXB2), a potent activator of platelet activation, increased by 27.4% in whole blood stimulated by endotoxin in the cold-exposed group, suggesting a prothrombotic state after cold exposure³⁷. Furthermore, we speculate that the changes in ICAM-3 and VEGF levels may be related to the activation of the renin-angiotensin system (RAS) in cold environments,

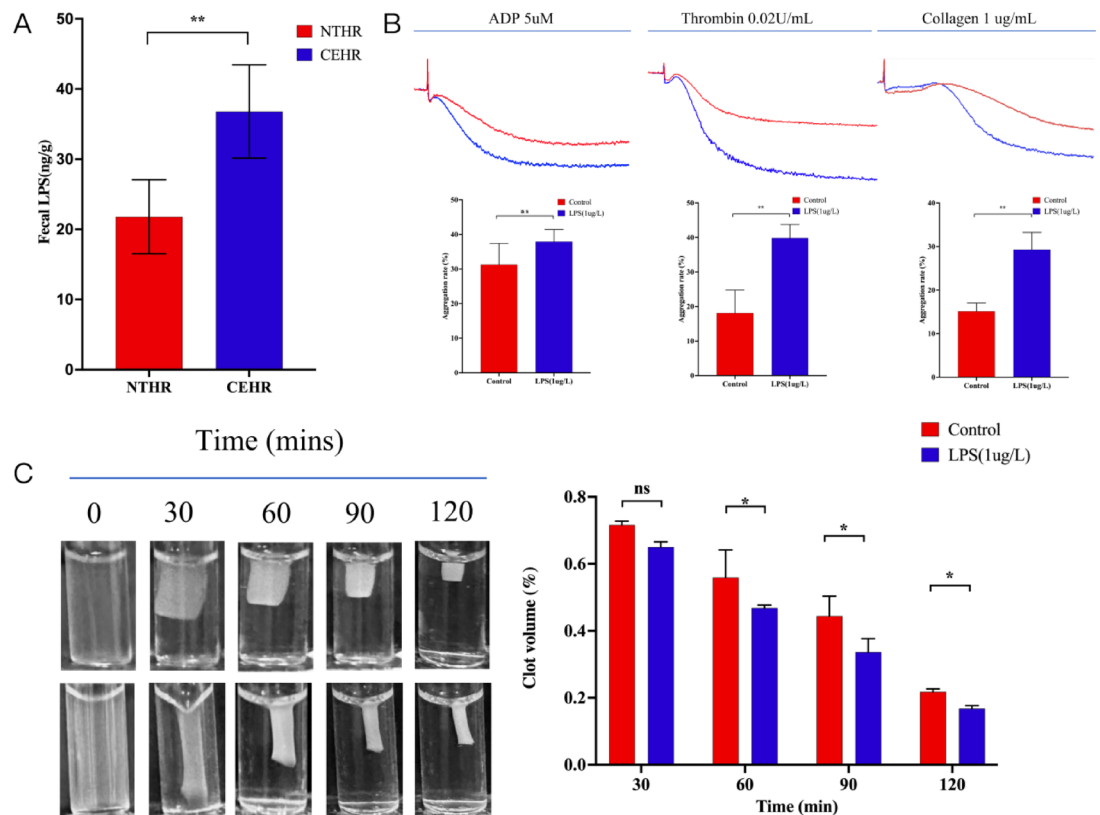


Fig. 9. (A) Levels of fecal LPS; (B) Effect of in vitro LPS incubation on platelet aggregation; (C) Effect of in vitro LPS incubation on platelet retraction. ns, not significant; * $P < 0.05$; ** $P < 0.01$.

leading to elevated levels of angiotensin II (ANG-II), which triggers inflammatory responses and vascular damage³⁸. We conducted an in-depth analysis of the systemic immune-inflammation index (SII). Although an increasing trend in the SII was observed in both the HR and LR groups, these changes did not reach statistical significance, which may be related to seasonal factors, particularly winter temperature fluctuations. The results of this study also showed that, in the HR group, the within-group β -diversity became more dispersed after the cold wave, suggesting a marked dysregulation of the gut microbiota. Overall, these findings indicate that the HR group is more sensitive to temperature fluctuations in cold environments and has a weaker capacity to maintain gut microbial homeostasis. We speculate that this phenomenon may be related to the resilience of the gut microbiota. The composition of the gut microbiota is influenced by both host and environmental factors. Although individuals are continuously exposed to environmental challenges in daily life, the gut microbiota typically maintains a relatively stable composition and function within the host due to its inherent resilience³⁹. However, individuals in the HR group may have a weaker baseline microbial homeostasis or impaired regulatory capacity, making them more prone to microbial imbalance under environmental stress, such as a cold wave. This leads to a higher sensitivity to low temperature exposure and more pronounced microbiota disturbances. In addition, homeostatic balance also plays an important role. The HR group often presents with comorbidities such as hypertension and diabetes, which can impair intestinal barrier function and disrupt immune regulation. These conditions may weaken the host's defense mechanisms against environmental stressors⁴⁰. As a result, their gut microbiota is more vulnerable to imbalance in response to environmental changes like cold waves, showing reduced stability and adaptability.

Although multiple studies have suggested a link between the gut microbiota and cold exposure⁴¹, it remains unclear whether the changes in the gut microbiota induced by cold exposure play a significant role in the development of IS. To fill this critical gap, we conducted experiments including gut microbiota analysis in human populations, antibiotic treatment in C57BL/6J mice, and fecal microbiota transplantation. Consistent with previous studies⁴², gut microbiota analysis of the human population revealed a decrease in the microbial richness of the HR group, with further dysregulation observed after the cold wave. Several bacteria potentially involved in the pathogenesis of ischemic stroke (IS) are altered. For example, the abundance of *Prevotella*₉ and *Romboutsia* increased, whereas that of *Anaerostipes* decreased. The *Prevotella* genus is associated with chronic inflammation, which may play an important role in hypertension⁴³, whereas *Anaerostipes* is closely related to short-chain fatty acid production⁴⁴, which can reduce the risk of IS.

To investigate whether changes in the gut microbiota are associated with increased stroke risk due to cold exposure, we conducted antibiotic treatment and fecal microbiota transplantation (FMT). After fecal transplantation, we detected increased platelet aggregation and clot retraction in the CEHR group of mice, as well as damage to the intestinal mucosal barrier. We speculate that these phenomena may be related to changes

in the intestinal microbiota composition and function of the two groups. Analysis of the intestinal microbiota composition of the two groups revealed that, during CEHR stroke, some inflammation-related microbes, including *s__Duncaniella_dubosii*, *s__Enterocloster_bolteae*, *s__Parabacteroides_distasonis*, *s__Anaerostipes_hominis*, and *s__Barnesiella_intestinihominis*, were significantly enriched^{45–48}. Using the KEGG database, we predicted the gene functions of the intestinal microbiota, which revealed that lipid metabolism and energy metabolism were more abundant in the CEHR group, which is consistent with the findings of previous studies⁴⁹. Changes in lipid metabolism affect the levels of TMAO. Further analysis revealed that genes involved in glycerophospholipid metabolism, sphingolipid metabolism, linoleic acid metabolism, arachidonic acid metabolism, and alpha-linolenic acid metabolism were significantly enriched in the CEHR group. Phosphatidylcholine, an important product of glycerophospholipid metabolism, is one of the precursors of TMAO. Previous studies have shown that TMAO accelerates the process of atherosclerosis and promotes platelet activation⁵⁰. Sphingolipid metabolism and linoleic acid metabolism also indirectly affect TMAO production through their impact on lipid metabolism. Arachidonic acid metabolism also plays an important role in platelet activation, aggregation, and thrombus formation. Additionally, the results revealed a significant increase in lipopolysaccharide biosynthesis in the CEHR group. LPS has a strong immunostimulatory effect, activating the host immune system, particularly through Toll-like receptor 4 (TLR4), leading to the release of inflammatory factors such as the tumor necrosis factor TNF- α and the interleukin IL-6, which damage intestinal epithelial cells, especially by disrupting the tight junctions between epithelial cells, thereby increasing intestinal barrier permeability. We also found that genes related to the production of short-chain fatty acids, such as those related to propanoate metabolism and the pentose phosphate pathway, were significantly enriched in the NTHR group. A reduction in short-chain fatty acids after cold exposure also increases the risk of cardiovascular and cerebrovascular diseases, which is consistent with previous study results.

In this study, we confirmed that cold exposure induces an increase in fecal LPS levels and validated, through in vitro experiments, the role of LPS in promoting platelet aggregation and clot retraction. However, the specific mechanisms by which LPS affects platelet protein activation—particularly whether it acts through receptor-dependent or receptor-independent pathways—and whether it interacts synergistically with other metabolic products remain to be further investigated.

This study systematically elucidates the important association between temperature stress-induced increases in the risk of stroke and intestinal microbiota disorders. The strength of this study is that, for the first time, we reported the associations between environmental temperature changes, the intestinal microbiota, and the risk of ischemic stroke, as validated by animal experiments, in a population-based study. Additionally, we used two temperature stress indicators: the Twenty-Four Solar Terms and specific meteorological data for time series grouping. Although the results are reliable, several limitations exist. Owing to insufficient data, this study focused primarily on the impact of cold environments on the intestinal microbiota and did not consider other environmental factors, such as PM_{2.5}, air pressure, and relative humidity. Future studies could consider the interactions among these factors. Given differences in living environments, future research could further stratify urban and rural populations. Moreover, previous studies noted that indoor temperatures fluctuate seasonally with outdoor temperatures but to a lesser extent, possibly related to heating and air conditioning systems. In areas with less heating, such as southern China, the correlation between the indoor and outdoor temperatures is stronger. When assessing the relationship between temperature and disease incidence, both indoor and outdoor temperatures should be considered, and a more comprehensive approach to explore the mechanisms of stroke incidence should be adopted. In future studies, lifestyle factors such as smoking and alcohol consumption should be included as covariates in microbiota analyses based on larger sample sizes, in order to more comprehensively control for potential confounding factors and enhance the robustness and interpretability of the findings.

Conclusion

In conclusion, cold exposure significantly increases the risk of ischemic stroke, particularly among high-risk stroke patients. This study provides preliminary evidence suggesting that cold exposure may promote the incidence of ischemic stroke by altering the composition and functionality of the gut microbiota. These findings offer important scientific support for research on stroke mechanisms as well as targeted interventions for disease prevention and treatment.

Data availability

All data generated and analyzed in this study are available from the corresponding author upon request. The 16S rRNA gene sequencing data generated in this study have been deposited in NCBI's Gene Expression BioProject under accession number PRJNA1208680.

Received: 14 January 2025; Accepted: 16 June 2025

Published online: 01 July 2025

References

- Morrison, S. F. & Nakamura, K. Central mechanisms for thermoregulation. *Annu. Rev. Physiol.* **81**, 285–308. <https://doi.org/10.1146/annurev-physiol-020518-114546> (2019).
- Tan, C. L. & Knight, Z. A. Regulation of body temperature by the nervous system. *Neuron* **98**(1), 31–48. <https://doi.org/10.1016/j.neuron.2018.02.022> (2018).
- Porvari, K., Horioka, K., Kaija, H. & Pakanen, L. Amphiregulin is overexpressed in human cardiac tissue in hypothermia deaths; associations between the transcript and stress hormone levels in cardiac deaths. *Ann. Med.* **56**(1), 2420862. <https://doi.org/10.1080/07853890.2024.2420862> (2024).

4. Chen, R. et al. Association between ambient temperature and mortality risk and burden: time series study in 272 main Chinese cities. *BMJ* **363**, 4306. <https://doi.org/10.1136/bmj.k4306> (2018).
5. Seki, T. et al. Brown-fat-mediated tumour suppression by cold-altered global metabolism. *Nature* **608**(7922), 421–428. <https://doi.org/10.1038/s41586-022-05030-3> (2022).
6. Stewart, S., Keates, A. K., Redfern, A. & McMurray, J. J. V. Seasonal variations in cardiovascular disease. *Nat. Rev. Cardiol.* **14**(11), 654–664. <https://doi.org/10.1038/nrcardio.2017.76> (2017).
7. Sugimoto, S. et al. Brown adipose tissue-derived MaR2 contributes to cold-induced resolution of inflammation. *Nat. Metab.* **4**(6), 775–790. <https://doi.org/10.1038/s42255-022-00590-0> (2022).
8. Burkart, K. G. et al. Estimating the cause-specific relative risks of non-optimal temperature on daily mortality: A two-part model modelling approach applied to the Global Burden of Disease Study. *Lancet* **398**(10301), 685–697. [https://doi.org/10.1016/S0140-6736\(21\)01700-1](https://doi.org/10.1016/S0140-6736(21)01700-1) (2021).
9. Rakers, F. et al. Rapid weather changes are associated with increased ischemic stroke risk: A case-crossover study. *Eur. J. Epidemiol.* **31**(2), 137–146. <https://doi.org/10.1007/s10654-015-0060-3> (2016).
10. Phung, D. et al. Heatwave and risk of hospitalization: A multi-province study in Vietnam. *Environ. Pollut.* **220**(Pt A), 597–607. <https://doi.org/10.1016/j.envpol.2016.10.008> (2017).
11. Gao, J. et al. The association between cold spells and admissions of ischemic stroke in Hefei, China: Modified by gender and age. *Sci. Total Environ.* **669**, 140–147. <https://doi.org/10.1016/j.scitotenv.2019.02.452> (2019).
12. Yin, P. et al. The added effects of heatwaves on cause-specific mortality: A nationwide analysis in 272 Chinese cities. *Environ. Int.* **121**(Pt 1), 898–905. <https://doi.org/10.1016/j.envint.2018.10.016> (2018).
13. Li, Z., He, X., Fang, Q. & Yin, X. Gut microbe-generated metabolite trimethylamine-N-oxide and ischemic stroke. *Biomolecules* **14**(11), 1463. <https://doi.org/10.1016/j.biom.2018.10.016> (2018).
14. Honarpisheh, P., Bryan, R. M. & McCullough, L. D. Aging microbiota-gut-brain axis in stroke risk and outcome. *Circ. Res.* **130**(8), 1112–1144. <https://doi.org/10.1161/CIRCRESAHA.122.319983> (2022).
15. Xu, K. et al. Rapid gut dysbiosis induced by stroke exacerbates brain infarction in turn. *Gut* **70**(8), 1486–1494. <https://doi.org/10.1136/gutjnl-2020-323263> (2021).
16. Chevalier, C. et al. Gut microbiota orchestrates energy homeostasis during cold. *Cell* **163**(6), 1360–1374. <https://doi.org/10.1016/j.cell.2015.11.004> (2015).
17. Wang, B. et al. Cold exposure, gut microbiota, and hypertension: A mechanistic study. *Sci. Total Environ.* **833**, 155199. <https://doi.org/10.1016/j.scitotenv.2022.155199> (2022).
18. Milsteyn, A., Colosimo, D. A. & Brady, S. F. Accessing bioactive natural products from the human microbiome. *Cell Host. Microbe* **23**(6), 725–736. <https://doi.org/10.1016/j.chom.2018.05.013> (2018).
19. Pletsch-Borba, L. et al. Vascular injury biomarkers and stroke risk: A population-based study. *Neurology* **94**(22), e2337–e2345. <https://doi.org/10.1212/WNL.0000000000009391> (2020).
20. Lin, J. et al. Association of Lp-PLA2-A and early recurrence of vascular events after TIA and minor stroke. *Neurology* **85**(18), 1585–1591. <https://doi.org/10.1212/WNL.0000000000001938> (2015).
21. Raffaele, S. et al. Microglial TNFR2 signaling regulates the inflammatory response after CNS injury in a sex-specific fashion. *Brain Behav. Immun.* **116**, 269–285. <https://doi.org/10.1016/j.bbi.2020.09.039> (2024).
22. Wang, H. J. et al. Catalpol improves impaired neurovascular unit in ischemic stroke rats by enhancing VEGF-PI3K/AKT and VEGF-MEK1/2/ERK1/2 signaling. *Acta Pharmacol. Sin.* **43**(7), 1670–1685. <https://doi.org/10.1038/s41401-021-00803-4> (2022).
23. Lu, F., Wang, Y., Miao, F., Han, C. & Meng, X. Rising incidence of acute epiglottitis in Eastern China: An eight-year retrospective study and its association with the 24 solar terms. *Int. J. Gen. Med.* **17**, 1665–1676. <https://doi.org/10.2147/IJGM.S458019> (2024).
24. Xu, S., Li, H., Wang, J., Lu, L. & Dai, Z. Relationship between meteorological factors and mortality in patients with coronavirus disease 2019: A cross-sectional study. *Heliyon* **9**(8), e18565. <https://doi.org/10.1016/j.heliyon.2023.e18565> (2023).
25. Kongwacharapong, J., Sornkhamphan, A., Kaveeta, C. & Nathisuwan, S. Validation and comparison of the stroke prognosis instrument (SPI-II) and the essen stroke risk score (ESRS) in predicting stroke recurrence in Asian population. *BMC Neurol.* **23**(1), 287. <https://doi.org/10.1186/s12883-023-03329-w> (2023).
26. Liu, G., Qian, H., Wang, L. & Wu, W. Systemic immune-inflammation index and its association with the prevalence of stroke in the United States population: A cross-sectional study using the NHANES database. *Rev. Cardiovasc. Med.* **25**(4), 130. <https://doi.org/10.31083/j.rcm2504130> (2024).
27. Huang, Y. W., Yin, X. S. & Li, Z. P. Association of the systemic immune-inflammation index (SII) and clinical outcomes in patients with stroke: A systematic review and meta-analysis. *Front. Immunol.* **13**, 1090305. <https://doi.org/10.3389/fimmu.2022.1090305> (2022).
28. Chen, Z. et al. Low ambient temperature exposure increases the risk of ischemic stroke by promoting platelet activation. *Sci. Total Environ.* **912**, 169235. <https://doi.org/10.1016/j.scitotenv.2023.169235> (2024).
29. Yang, J. et al. PIM1-HDAC2 axis modulates intestinal homeostasis through epigenetic modification. *Acta Pharm. Sin. B.* **14**(7), 3049–3067. <https://doi.org/10.1016/j.apsb.2024.04.017> (2024).
30. Jeong, S., Davis, C. K. & Vemuganti, R. Mechanisms of time-restricted feeding-induced neuroprotection and neuronal plasticity in ischemic stroke as a function of circadian rhythm. *Exp. Neurol.* **383**, 115045. <https://doi.org/10.1016/j.apsb.2024.04.017> (2025).
31. Kanehisa, M., Furumichi, M., Sato, Y., Matsuura, Y. & Ishiguro-Watanabe, M. KEGG: Biological systems database as a model of the real world. *Nucleic Acids Res.* **53**(D1), D672–D677. <https://doi.org/10.1093/nar/gkac909> (2025).
32. Kanehisa, M. Toward understanding the origin and evolution of cellular organisms. *Protein Sci.* **28**(11), 1947–1951. <https://doi.org/10.1002/pro.3715> (2019).
33. Ogata, H. et al. KEGG: Kyoto encyclopedia of genes and genomes. *Nucleic Acids Res.* **27**(1), 29–34. <https://doi.org/10.1093/nar/27.1.29> (1999).
34. Li, X. et al. Global, regional, and national temporal trends in mortality and disability-adjusted life years for cardiovascular disease attributable to low temperature during 1990–2019: An age-period-cohort analysis of the global burden of disease 2019 study. *Front. Public Health* **12**, 1414979. <https://doi.org/10.3389/fpubh.2024.1414979> (2024).
35. Xue, J. et al. Seasonal variation in neurological severity and clinical outcomes in ischemic stroke patients - A 9-year study of 5238 patients. *Circ. J.* **87**(9), 1187–1195. <https://doi.org/10.1253/circj.CJ-22-0801> (2023).
36. Sun, X. et al. Seasonal variability of lesions distribution in acute ischemic stroke: A retrospective study. *Sci. Rep.* **14**(1), 11831. <https://doi.org/10.1038/s41598-024-62631-w> (2024).
37. Zafeiratou, S. et al. A systematic review on the association between total and cardiopulmonary mortality/morbidity or cardiovascular risk factors with long-term exposure to increased or decreased ambient temperature. *Sci. Total Environ.* **772**, 145383. <https://doi.org/10.1016/j.scitotenv.2021.145383> (2021).
38. Chen, Z., Liu, P., Xia, X., Wang, L. & Li, X. The underlying mechanisms of cold exposure-induced ischemic stroke. *Sci. Total Environ.* **834**, 155514. <https://doi.org/10.1016/j.scitotenv.2022.155514> (2022).
39. Sommer, F., Anderson, J. M., Bharti, R., Raes, J. & Rosenstiel, P. The resilience of the intestinal microbiota influences health and disease. *Nat. Rev. Microbiol.* **15**(10), 630–638. <https://doi.org/10.1038/nrmicro.2017.58> (2017).
40. Yang, Z. et al. Gut microbiota and hypertension: Association, mechanisms and treatment. *Clin. Exp. Hypertens.* **45**(1), 2195135. <https://doi.org/10.1080/10641963.2023.2195135> (2023).

41. Bercik, P. et al. The intestinal microbiota affect central levels of brain-derived neurotropic factor and behavior in mice. *Gastroenterology* **141**(2), 599–609. <https://doi.org/10.1053/j.gastro.2011.04.052> (2011).
42. Worthmann, A. et al. Cold-induced conversion of cholesterol to bile acids in mice shapes the gut microbiome and promotes adaptive thermogenesis. *Nat. Med.* **23**(7), 839–849. <https://doi.org/10.1038/nm.4357> (2017).
43. Li, J. et al. Gut microbiota dysbiosis contributes to the development of hypertension. *Microbiome* **5**(1), 14. <https://doi.org/10.1186/s40168-016-0222-x> (2017).
44. Niu, X. et al. Effect of oral metformin on gut microbiota characteristics and metabolite fractions in normal-weight type 2 diabetic mellitus patients. *Front. Endocrinol. (Lausanne)* **15**, 1397034. <https://doi.org/10.3389/fendo.2024.1397034> (2024).
45. Liu, Y. et al. Augmented temperature fluctuation aggravates muscular atrophy through the gut microbiota. *Nat. Commun.* **14**(1), 3494. <https://doi.org/10.1038/s41467-023-39171-4> (2023).
46. Wang, L. et al. Fucoidan ameliorates alcohol-induced liver injury in mice through Parabacteroides distasonis-mediated regulation of the gut–liver axis. *Int. J. Biol. Macromol.* **279**(Pt 3), 135309. <https://doi.org/10.1016/j.ijbiomac.2024.135309> (2024).
47. Sprotte, S., Brinks, E., Neve, H. & Franz, C. Complete genome sequence of the novel virulent phage PMBT24 infecting *Enterocloster boltea* from the human gut. *Heliyon* **10**(8), e28813. <https://doi.org/10.1016/j.heliyon.2024.e28813> (2024).
48. Lan, Y. W. et al. Kefir peptides mitigate bleomycin-induced pulmonary fibrosis in mice through modulating oxidative stress, inflammation and gut microbiota. *Biomed. Pharmacother.* **174**, 116431. <https://doi.org/10.1016/j.biopha.2024.116431> (2024).
49. Bornstein, M. R. et al. Comprehensive quantification of metabolic flux during acute cold stress in mice. *Cell Metab.* **35**(11), 2077–2092.e2076. <https://doi.org/10.1016/j.cmet.2023.09.002> (2023).
50. Ronen, D. et al. Human gut microbiota in cardiovascular disease. *Compr. Physiol.* **14**(3), 5449–5490. <https://doi.org/10.1002/cphy.c230012> (2024).

Acknowledgements

The authors thank all the study participants, staff of the participating hospitals.

Author contributions

Xin Li: Conceptualization, Investigation—original draft, Visualization. Zhou Xiao: Conceptualization, Investigation, Writing—original draft. Chanjuan Wei: Writing—review & editing, Supervision. Jiaming Liu: Writing—review & editing, Supervision. Xiaoshuang Xia: Writing—review & editing, Supervision. Lin Wang: Writing—review & editing, Supervision.

Funding

This work was supported by the Tianjin Municipal Science and Technology Bureau Project (21JCZDJC01230), the Key Projects of Tianjin Municipal Health Commission (TJWJ2023XK007), the Tianjin Key Medical Discipline (Specialty) Construction Project (TJYXZDXK-065B), the Tianjin Center for Health and Meteorology Multidisciplinary Innovation, and the National Natural Science Foundation of China (42275197).

Declarations

Competing interest

The authors declare no competing interests.

Ethical approval

This study was approved by the Ethics Committee of the Second Hospital of Tianjin Medical University (Approval No. KS20220901). This study follows the relevant guidelines and regulations (), and all experiments were conducted under conditions that comply with ethical requirements.

Additional information

Supplementary Information The online version contains supplementary material available at <https://doi.org/10.1038/s41598-025-07614-1>.

Correspondence and requests for materials should be addressed to X.L.

Reprints and permissions information is available at www.nature.com/reprints.

Publisher's note Springer Nature remains neutral with regard to jurisdictional claims in published maps and institutional affiliations.

Open Access This article is licensed under a Creative Commons Attribution-NonCommercial-NoDerivatives 4.0 International License, which permits any non-commercial use, sharing, distribution and reproduction in any medium or format, as long as you give appropriate credit to the original author(s) and the source, provide a link to the Creative Commons licence, and indicate if you modified the licensed material. You do not have permission under this licence to share adapted material derived from this article or parts of it. The images or other third party material in this article are included in the article's Creative Commons licence, unless indicated otherwise in a credit line to the material. If material is not included in the article's Creative Commons licence and your intended use is not permitted by statutory regulation or exceeds the permitted use, you will need to obtain permission directly from the copyright holder. To view a copy of this licence, visit <http://creativecommons.org/licenses/by-nc-nd/4.0/>.

© The Author(s) 2025